
GAMMA-LOUD BINARIES

Final Degree Project

Author

Sabina Monzón Navarro

Supervised by

Alicia López Oramas

La Laguna, July 8, 2023

Grado en Física, Facultad de Ciencias

Universidad de La Laguna

Instituto de Astrofísica de Canarias

Agradecimientos

El Grado en Física ha sido uno de los mayores retos que he enfrentado hasta ahora. En estos años de adquirir tanto conocimiento he encontrado muchos obstáculos en el camino que he sorteado con éxito, ya que hoy, 8 de julio de 2023, entrego mi Trabajo de Fin de Grado. Pero ese éxito no hubiera sido posible sin el apoyo de varias personas, a las que me gustaría dedicar unas palabras de agradecimiento.

Gracias a mi tutora, Alicia, por dirigir este trabajo y mis prácticas externas. Me has dado la oportunidad de adquirir un amplio conocimiento sobre los sistemas que se estudian a altas energías y de hablar con más investigadores relacionados con este ámbito durante el periodo de prácticas. Siempre me has recibido con una sonrisa en cada reunión y me has animado y apoyado durante este último año, lo cual te agradeceré siempre.

Gracias a mis amigos (que no compañeros, ellos saben por qué lo digo) de *La Posada*. En el primer año de carrera fue una sorpresa encontrar a tantas personas maravillosas con las que me podía sentir como en casa estando tan lejos de ella, y que hoy en día se siguen riendo con mis frases célebres como “Soy pan” o “El queso tiene café”.

Gracias a Micaela, por apoyarme siempre, aunque solo nos veamos una vez al año. Sabes que para mí siempre serás mi mejor amiga.

Gracias a Chacho, por escucharme, confiar en mí y ayudarme siempre que lo he necesitado. Especialmente, gracias por este último año, en el que no hemos podido vernos tanto como nos gustaría, pero nunca has dejado de ser mi refugio, mi lugar seguro, por muy lejos que estés. Te quiero, gracias por ser mi compañero de vida.

Por último, gracias a mis padres y a mi hermano por confiar siempre en mí y apoyarme de manera incondicional desde que decidí estudiar el Grado en Física. Aunque he estado lejos de casa, siempre los he sentido a mi lado. Los quiero.

Contents

1. Resumen
2. Introduction
3. Objectives and methodology
4. Gamma-ray binaries
5. Gamma-ray emitting binaries
 - 5.1. Microquasars
 - 5.2. Colliding wind binaries
 - 5.3. Novae
6. The MAGIC telescopes and introduction to data analysis
7. Data analysis, results, and discussion
 - 7.1. Data analysis of the gamma-ray binary *PSR J2032+4127*
 - 7.1.1. Signal evaluation
 - 7.1.2. Skymap
 - 7.1.3. Spectral energy distribution (SED) and lightcurve
 - 7.2. Evaluation of the gamma-ray binary candidate *HESS J1828-099* for MAGIC observations.
8. Conclusions
9. References

1. Resumen

Un sistema binario es aquel compuesto por dos cuerpos que orbitan entre sí. Muchos de estos sistemas han sido detectados en frecuencias de radio, ópticas y de rayos X. Entre los años 70 y 90, el descubrimiento de binarias de rayos X coincidentes con radio púlsares que emiten radiación no térmica fue un indicio de que estos sistemas podían ser detectados como emisores de rayos gamma [1]. En los últimos 20 años, el desarrollo y mejora de telescopios Cherenkov, que detectan indirectamente rayos gamma de muy alta energía ($E > 100$ GeV) a través de la emisión de radiación Cherenkov en la atmosfera, así como la contribución de satélites de rayos gamma, que son sensibles a energías mayores que 100 MeV, han permitido el descubrimiento de muchos sistemas binarios que denominamos binarias brillantes en gamma (gamma-loud binaries en inglés).

En la introducción de este trabajo explicamos que las binarias brillantes en gamma son todas aquellas en las que se han detectado rayos gamma de muy altas energías (VHE por sus siglas en inglés: $E > 100$ GeV) y/o altas energías (HE por sus siglas en inglés: 100 MeV $< E < 100$ GeV). Estos sistemas binarios, a su vez, se pueden clasificar en dos sub-clases: las históricamente conocidas como binarias de rayos gamma (gamma-ray binaries en inglés), que fueron las primeras descubiertas y que presentan un pico característico por encima de 1 MeV en sus distribuciones de energía espectral y las binarias emisoras de rayos gamma (gamma-ray emitting binaries en inglés), que presentan distribuciones de energía espectral totalmente diferentes y cuya emisión de rayos gamma ha sido descubierta recientemente, creando la necesidad de identificarlas como una clase diferente a la anterior. También analizamos los primeros modelos propuestos teniendo en cuenta que las binarias de rayos gamma están constituidas por un objeto compacto, que puede ser un agujero negro o una estrella de neutrones, orbitando alrededor de una estrella compañera. Explicamos también los distintos mecanismos por los que se producen rayos gamma, que se corresponden con radiación no térmica. Por último, incluimos algunas definiciones útiles, como los conceptos de significancia, mapa del cielo, distribución de energía espectral y curva de luz.

En el capítulo 3 explicamos los objetivos de este trabajo y el procedimiento que se ha seguido. Teniendo en cuenta el contexto proporcionado en la introducción, el primer objetivo es proporcionar una clasificación de las binarias brillantes en gamma conocidas hasta ahora, para lo que se realiza una exhaustiva búsqueda bibliográfica. El segundo objetivo es familiarizarse con los pasos finales del proceso de análisis de datos de los telescopios Cherenkov MAGIC, para lo que se estudia la binaria de rayos gamma *PSR J2032+4127*. Finalmente, se evalúa si la candidata a binaria de rayos gamma *HESS J1828-099* puede ser detectada con MAGIC. Para estos análisis se utilizan diferentes programas proporcionados por los miembros de esta colaboración.

En el capítulo 4 profundizamos en las binarias de rayos gamma. Se muestra la distribución de energía espectral propia de estos sistemas, así como algunas características comunes. Esta sub-clase de binarias brillantes en gamma presentan patrones similares en la emisión de rayos X y en radio. Sin embargo, cada binaria de rayos gamma presenta sus propias características en la emisión gamma, detectada tanto a altas como a muy altas energías. Por ello, profundizamos en las principales características de las 8 binarias de este tipo descubiertas hasta ahora y mostramos una tabla en la que recogemos algunos de los parámetros que las describen, como la distancia a la que se encuentran respecto a un observador en La Tierra, en qué fases de la órbita emiten rayos gamma, entre otras. Por

último, mencionamos algunas de las cuestiones pendientes de resolver de esta sub-clase de binarias brillantes en gamma.

En el capítulo 5 profundizamos en las binarias emisoras de rayos gamma. Se muestra que presentan una distribución de energía espectral diferente a la obtenida para las binarias de rayos gamma. En esta categoría, encontramos microcuásares, binarias de viento en colisión, y novas. Los microcuásares son sistemas binarios alimentados por objetos compactos (agujeros negros o estrellas de neutrones) a través de la acreción de masa de una estrella compañera, lo que genera chorros de partículas relativistas. En el apartado correspondiente se detallan las características principales de los microcuásares detectados a altas y/o muy altas energías. Por su parte, las binarias de viento en colisión están formadas por dos estrellas masivas, por lo que son las únicas binarias brillantes en gamma que no contienen un objeto compacto. Los rayos gamma se producen en la región de interacción entre los vientos estelares. La única firmemente detectada en el rango de rayos gamma es Eta Carinae, por lo que nos centramos en explicar sus características principales. Por último, las novas son sistemas binarios que presentan una transferencia de masa de una estrella compañera a una enana blanca, lo que produce explosiones termonucleares en la superficie de la enana blanca. En este trabajo nos centramos en la nova RS Ophiuchi, la primera descubierta en el rango de rayos gamma de muy altas energías.

En el capítulo 6 se detallan las características principales de MAGIC, que son dos telescopios Cherenkov situados en el Observatorio del Roque de los Muchachos, en La Palma, que detectan rayos gamma desde 50 GeV hasta 100 TeV. También se introducen los distintos niveles de reconstrucción de los datos obtenidos con estos telescopios, con el objetivo de familiarizarnos con el procedimiento general para centrarnos en el último nivel del análisis en el capítulo 7.

El capítulo 7 se divide en dos apartados: el primero de ellos se corresponde con el análisis de alto nivel de 8.21 horas de datos de buena calidad obtenidos para la binaria de rayos gamma *PSR J2032+4127*, con el fin de evaluar la señal observada, obtener su mapa de cielo y calcular la distribución de energía espectral y la curva de luz. Los resultados obtenidos se comparan con los publicados en [32] para comprender mejor las propiedades de esta binaria y evaluar si coinciden dentro de las incertidumbres experimentales. En el segundo apartado, nos centraremos en evaluar si la candidata a binaria de rayos gamma *HESS J1828-099* se podría detectar con los telescopios MAGIC y cuánto tiempo de observación sería necesario para obtener un espectro de calidad. Concluimos que las distribuciones de energía espectral simuladas nos permiten plantear una propuesta observacional con estos telescopios.

Por último, en el capítulo 8, extraemos las conclusiones teniendo en cuenta lo estudiado en los capítulos previos.

2. Introduction

La detección de sistemas binarios que emiten rayos gamma se ha logrado con telescopios Cherenkov y satélites de rayos gamma en los últimos 20 años. En este capítulo, se estudia desde un punto de vista histórico el descubrimiento de las primeras binarias de rayos gamma, que con el transcurso del tiempo se han clasificado como miembros pertenecientes a una familia heterogénea conocida como binarias brillantes en gamma. También se analizan los principales mecanismos por los que pueden emitir rayos gamma y se definen los conceptos necesarios para el análisis de estos sistemas.

A binary system is composed of two bodies orbiting each other. Many of these systems have been identified as powerful radio, optical, and X-ray emitters [1]. Between the 70s and the 90s, the discovery of X-ray binaries coincident with radio pulsars emitting non-thermal radiation was a hint that these sources could potentially be gamma-ray emitters. In the 2000s, the development of the third generation of Imaging Atmospheric Cherenkov Telescopes (IACTs) [2], which indirectly detect gamma rays through the emission of Cherenkov radiation in the atmosphere thanks to their high sensitivities and better angular and energy resolution, allowed the discovery of the first gamma-ray binary, *PSR B1259-63* [3].

During these first years of operations of IACTs, the first three gamma-ray binaries were discovered. The second one was *LS 5039* [4], and the third one was *LS I+61°303* [5]. These systems have in common that are composed of a compact object with an eccentric orbit around a companion star. These binaries are so-called compact binaries and verify the following orbital definitions [6]:

- **Compact object:** a celestial body of very high density and mass that is the remnant of an initial star that evolves and dies. It can either be a black hole (BH) when the mass of the initial star (M) is $M \geq 10 - 25 M_{\odot}$, or a neutron star (NS) when $M \leq 10M_{\odot}$.
- **Companion star:** is the optical star which losses mass into the compact object. It can also be called mass-donor star.
- **Periastron:** is the point in the orbit in which the distance between the compact object and the companion star is minimum.
- **Apastron:** is the point in the orbit in which the distance between the compact object and the companion star is maximum.
- **Inferior conjunction (INFC):** is the point in the orbit in which the compact object is in front of the star which is orbiting, over the line of sight of an external observer located on Earth.
- **Superior conjunction (SUPC):** is the point in the orbit in which the compact object is in behind of the star which is orbiting, over the line of sight of an external observer located on Earth.

Figure 1 shows a scheme for a better understanding of these definitions.

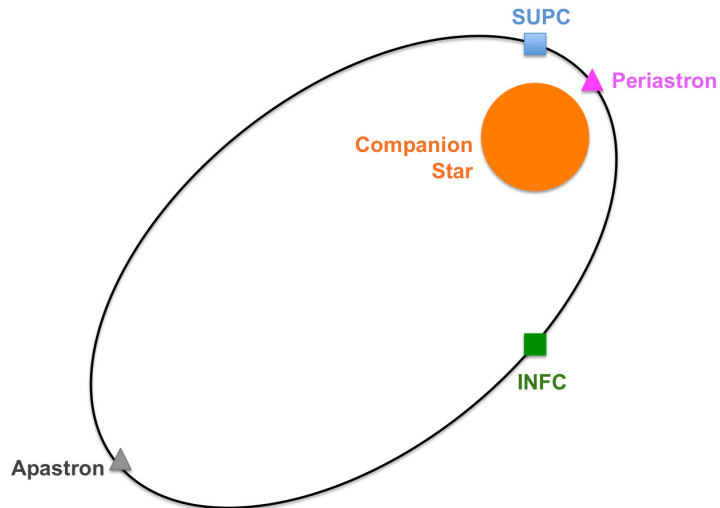


Figure 1: General orbital scheme of a binary system, in which the companion star is the orange circle, and the orbit of the compact object is represented in black. The periastron (pink triangle), the apastron (grey triangle), the SUPC (blue square), and the INFC (green square) are also represented. Credit: A. López Oramas.

At the time of the discovery of the first three gamma-ray binaries, only the nature of the compact object of *PSR B1259-63*, which is a pulsating neutron star (pulsar), was known. However, it was known that the compact objects of *LS 5039* and *LS I+61°303* had no more than 4 solar masses, which is compatible with a neutron star or a low-mass black hole. Considering it, two models were proposed to explain the emission of gamma rays from these binaries [7], as displayed in Figure 2:

- Microquasar-jet model: microquasars are powered by compact objects (NS or stellar-mass BH) via mass accretion from a companion star. This produces collimated jets that, if aligned with the light of sight of the observer, appear as microblazars. The jets boost the energy of the stellar photons to the range of very-energetic gamma rays.
- Pulsar-wind model: pulsar winds are powered by the rotation of neutron stars; the wind flows away to large distances in a comet-shape tail. The interaction of this wind with the companion-star outflow produces very-energetic gamma rays.

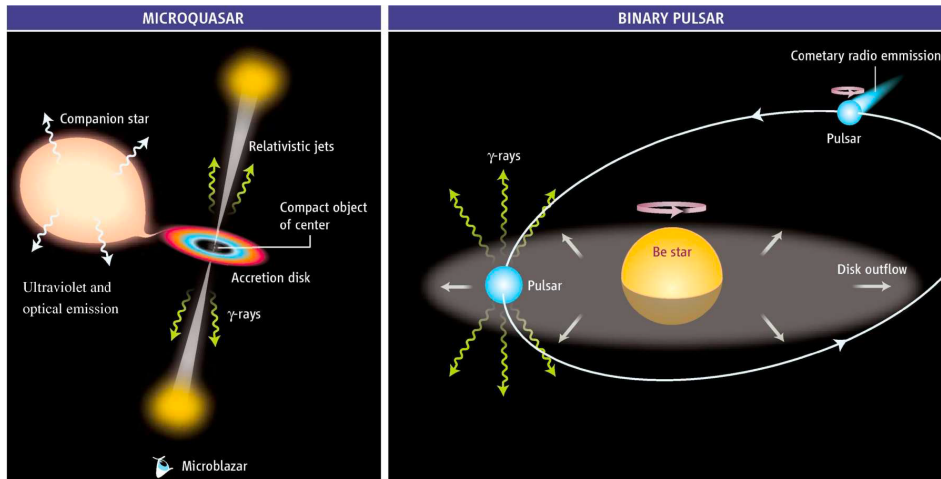


Figure 2: Models for very energetic gamma-ray binaries. Left: Microquasar-jet model. Right: Pulsar-wind model. Taken from [7].

In the last decade, the astrophysical research and the contribution and improvement of the IACTs and gamma-ray satellites have made it possible to detect more binaries that emit gamma rays and to confirm that not all these binaries follow the models of Figure 2, and not all are composed of a compact object. Thus, a classification of these binary systems is required.

Historically, what has been defined as gamma-ray binaries are those systems that present a characteristic peak above or approximately equal to 1 MeV in the spectral energy distribution (SED) [8]. However, over the past few years, other systems also emitting gamma-rays but with a different SED have been identified. We can define these systems as gamma-ray emitting binaries, which include microquasars, novae, and colliding wind binaries. Thus, these binary systems are two sub-classes of the currently named gamma-loud, which emits high-energy (HE, $100 \text{ MeV} < E < 100 \text{ GeV}$) and/or very-high-energy (VHE, $E > 100 \text{ GeV}$) gamma rays. The description of these systems is detailed in Chapters 4 and 5.

Besides, the study of the primary particles that produced the gamma rays is important for a better understanding of these gamma-loud binaries. Gamma rays are produced due to non-thermal processes, which are not described by black-body radiation. Two possible scenarios are involved in this production: a leptonic scenario, in which the primary particles have a leptonic origin (electrons or positrons), and a hadronic scenario, in which protons and ions are the parent particles. It is known that the most important mechanisms of the production of gamma rays in astrophysics are [6]:

- Inverse Compton scattering (IC): a relativistic electron scatters up a low-energy photon, transferring part of this energy and producing a gamma-ray. The parent particle is an electron, so this process belongs to the leptonic scenario. It requires an ambient with a radiation field and an environment transparent to gamma ray to allow them to scape from the production region. Typical photons are those

from stars, cosmic microwave background or synchrotron radiation. In the microquasar-jet model and the pulsar-wind model represented in Figure 2, the gamma rays are produced by this mechanism.

- Synchrotron radiation: electromagnetic radiation produced by relativistic electrons moving in a magnetic field. So, the parent particles have a leptonic origin. In general, the energy of the generated photons is less than that of the parent electrons, but in some astrophysical environments, gamma-ray emission can be produced. Strong magnetic fields are required. Also, synchrotron radiation may be a source of seed photons for the IC scattering.
- Bremsstrahlung: radiation emitted by the deceleration of an electron when it is deflected in the electrostatic field produced by a nucleus or ion. The process belongs to the leptonic scenario. In a non-relativistic regime, the gamma rays emitted will have the same spectrum as the electron acceleration spectrum, a power law. It requires an ambient with matter.
- Pion (π^0) decay: the interaction of a population of protons (or ions) through inelastic scattering with ambient gas can produce mesons (π). The neutral pion π^0 , which is produced with a probability of $\sim 30\%$ and has a short lifetime ($\sim 10^{-17} s$), decays into two gamma rays. So, the production of gamma rays in this case has a hadronic origin. Jets in microquasars can have a hadronic component, and it has recently been shown that novae are also proton accelerators.

Finally, the following concepts, which are more deeply explained in Chapter 7, allow us to study the individual and common properties of gamma-loud binaries:

- Significance (σ): parameter used to determine if a source is detected. In gamma-ray astronomy, a source detection is considered when the minimum value of the significance is 5σ .
- Skymap: plot of significance that gives information about the extension and spatial distribution of the source and the arrival direction of the incoming gamma rays.
- Spectral energy distribution (SED): plot which represents the energy flux per interval of energy.
- Lightcurve: plot which represents the evolution of the total energy flux over time.

3. Objectives and methodology

El primer objetivo de este trabajo es proporcionar una clasificación de las diferentes binarias brillantes en gamma conocidas hasta ahora. En este capítulo, se describen también los objetivos experimentales asociados a este trabajo, así como los métodos utilizados para lograrlos.

The first purpose of this work is to provide a classification of the different known gamma-loud binary systems and to describe their main characteristics. With that objective, we perform exhaustive bibliographic research, and we present our results in Chapter 4 about gamma-ray binaries and Chapter 5 about gamma-ray emitting binaries.

The second goal of this work is to get acquainted with the main features and the analysis technique of the MAGIC telescopes (Major Atmospheric Gamma-ray Imaging Cherenkov telescopes). Specifically, we work on the high-level data reconstruction, the final step of the process in which we obtain the signal evaluation, the skymap, the SED and the lightcurve of the gamma-ray binary *PSR J2032+4127* making use of MARS (MAGIC Analysis and Reconstruction Software) routines.

Furthermore, we made use of the MAGIC Source Simulator (MSS), provided by the MAGIC collaboration, to evaluate if the gamma-ray binary candidate *HESS J1828-099* can be detectable with high significance with the MAGIC telescopes, to understand how to prepare for an observational proposal. In Chapters 6 and 7 we delve into these analyzes.

Finally, in Chapter 8, we draw some conclusions about gamma-loud binaries considering what we have investigated and presented in previous chapters.

4. Gamma-ray binaries.

Las binarias de rayos gamma son aquellas que muestran un pico de emisión no térmica superior a 1 MeV en sus distribuciones de energía espectral. En este capítulo se estudian las características principales de las 8 binarias de rayos gamma detectadas hasta ahora, así como algunas cuestiones sobre estos sistemas que no se han logrado resolver.

Gamma-ray binaries are systems in which the non-thermal emission peaks at energies greater than 1 MeV in their SEDs. This means that most of the non-thermal emission is in the gamma-ray domain (see Figure 3).

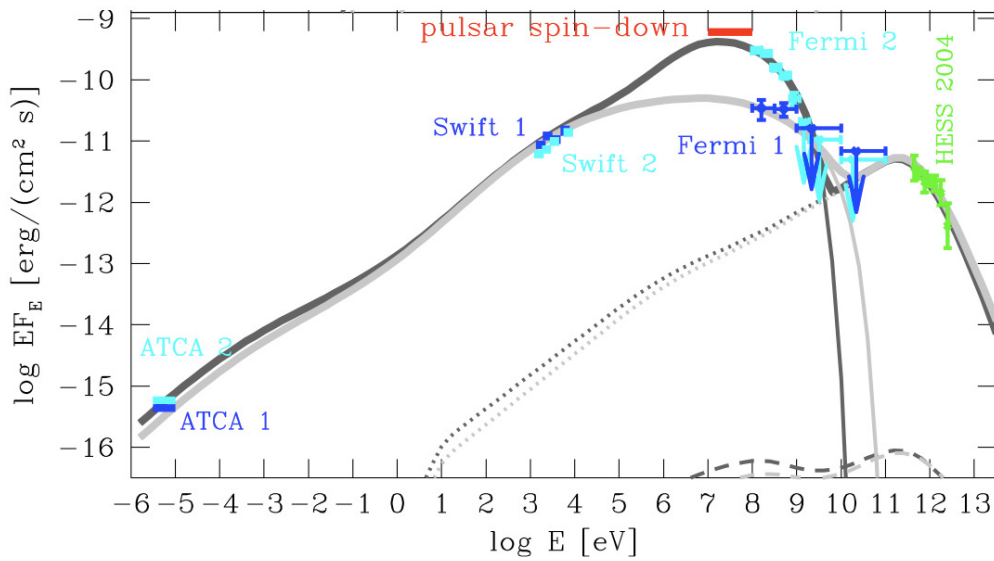


Figure 3: SED of PSR B1259-63. The peak of the non-thermal emission is released at high energies, above $\log(8)$, located in the gamma-ray domain. This is an intrinsic feature of the gamma-ray binaries. SED taken from [9].

These binary systems are composed of a BH or a NS orbiting a companion star. Depending on the absence or presence of a circumstellar disk in the companion star, two sub-groups can be defined respectively: those composed of an O or B star; and those composed of Be-type star. In the case of O or B stars, the lightcurve corresponding to the binary presents a single-peak profile, and the peak location along the orbit depends on the geometrical characteristics of the system. If the companion star is a type Be, depending on the orientation of the circumstellar disk and the orbital plane, several peaks can be displayed in the lightcurve and they could be correlated with the times in which the compact object crosses the star's circumstellar disk [8]. Figure 4 shows examples of these two types of gamma-ray binaries with different types of companion stars.

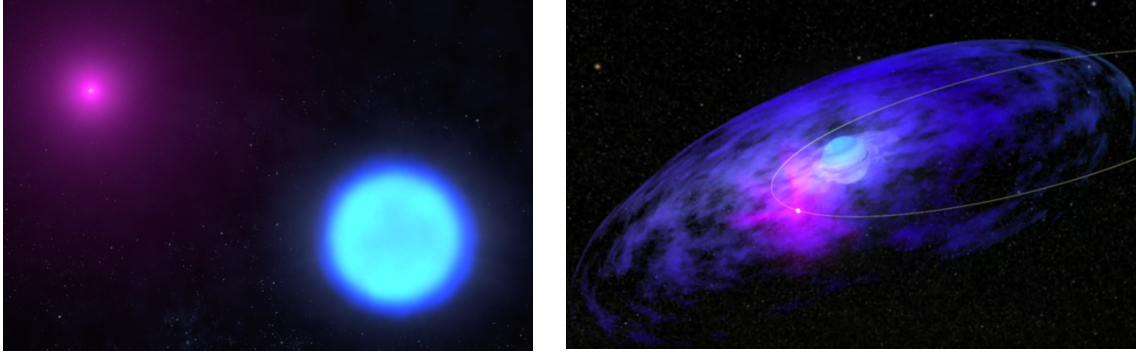


Figure 4: Left: illustration of LMC P3, a gamma-ray binary in which the companion star (blue) is a type O star with no circumstellar disk. Right: illustration of a gamma-ray binary in which the mass-donor star has a circumstellar disk, such as the case of LS I+61°303 due to the orientation of the circumstellar disk (blue) with respect to the orbital plane (grey). Credit: NASA.

In addition, gamma-ray binaries show non-thermal radio emission and a hard X-ray spectrum with moderated X-ray fluxes. These features make these systems different from high-mass X-ray binaries (which are also composed of a massive star and a compact object), which rarely show radio emission, have higher X-ray fluxes, present X-ray pulsations, and have a different SED [6].

Eight gamma-ray binaries have been so far confirmed as sources of both HE and VHE gamma rays. This non-thermal emission has been detected periodically along the orbit or, at least, during certain parts [6]. Table 1 contains a summary of the main characteristics of these systems, with a description ordered by date of discovery, from the first to the most recent.

<i>Gamma-ray binary</i>	<i>Star spectral type</i>	<i>Compact object</i>	<i>Star mass [M_{\odot}]</i>	<i>Distance [kpc]</i>	<i>P_{orb}</i>	<i>HE γ-ray emission</i>	<i>VHE γ-ray emission</i>
PSR B1259–63	Be	48 ms pulsar	31	2.3	~3.4 yrs	~Periastron	Periastron
LS 5039	O	-	23	2.5	3.9 d	Superior conjunction	Inferior conjunction
LS I+61°303	Be	0.27 s pulsar	12	2.0	26.5 d	Periastron	Apastron
HESS J0632+057	Be	-	16	1.5	316.7 d	yes	~Apastron
1FGL J1018.6–5856	O	-	31	6.4	16.5 d	Inferior conjunction	Inferior conjunction
LMC–P3	O	-	25-42	~50	10.3 d	~Superior conjunction	Inferior conjunction
PSR J2032+4127	Be	143 ms pulsar	15	1.4-1.7	~ 50 yrs	Periastron	~Periastron
HESS J1832–093	-	-	-	~4.4	86 d	yes	yes

Table 1: Parameters of the gamma-ray binaries so far known. From left to right, the quoted parameters are the gamma-ray binary, its star spectral type, its compact object if it is known, the star mass [in solar masses], the distance between the system and The

Earth [in kpc], the orbital period of the binary system, and the phases where HE and VHE γ -ray emissions take place.

PSR B1259-63

This gamma-ray binary was the first binary system to be detected in the gamma-ray domain [3]. Due to its location in the Southern Hemisphere, *PSR B1259-63* was detected by the Cherenkov telescopes of the H.E.S.S. (High Energy Stereoscopic System) experiment [10], located in Namibia. It is formed by a 48 ms pulsar (PSR), which was detected by radio-pulsar search [3], orbiting a massive Be star, LS 2883, in a highly eccentric orbit. The Be stellar disk is almost perpendicular to the orbital plane, so that the pulsar crosses the disk twice per orbit [11]. The VHE gamma-ray emission is detected in the vicinity of the periastron (close to superior conjunction). The HE gamma-ray emission is also detected in the vicinity of the periastron. The orbital period is about 3.4 years [3].

Currently, one of the most unusual features of this system is a bright HE flare that occurs 30-40 days after the periastron. This outburst has been detected recursively, carrying a significant fraction of the pulsar spin-down power [11]. To explain the luminosity of the HE flare and the absence of counterparts at other wavelengths, a model was proposed [12] in which the TeV and X-ray emission is generated by the strongly accelerated electrons of the pulsar wind (IC and synchrotron emission correspondingly). The HE emission in this model is a result of the IC emission of the unshocked and weakly shocked electrons, with a possible addition of bremsstrahlung emission on the clumps of the stellar wind material which penetrated beyond the shock cone. The luminosity of the HE flares within this model can be understood if the initially isotropic pulsar wind after the shock is reversed and confined within a cone looking, during the flare, in the direction of the observer [11].

In the periastron passage of 2021, the observation of a substantial delay in the rise of the HE emission, which started 55 days after the periastron, and unusual behavior in the X-ray band, in which a third flux peak appears 30 days after the periastron, can be explained within the model of IC and bremsstrahlung with the assumption that the outer parts of the Be star's disk are characterized by lower densities in comparison to previous periastron passages [11]. These results are displayed in Figure 5.

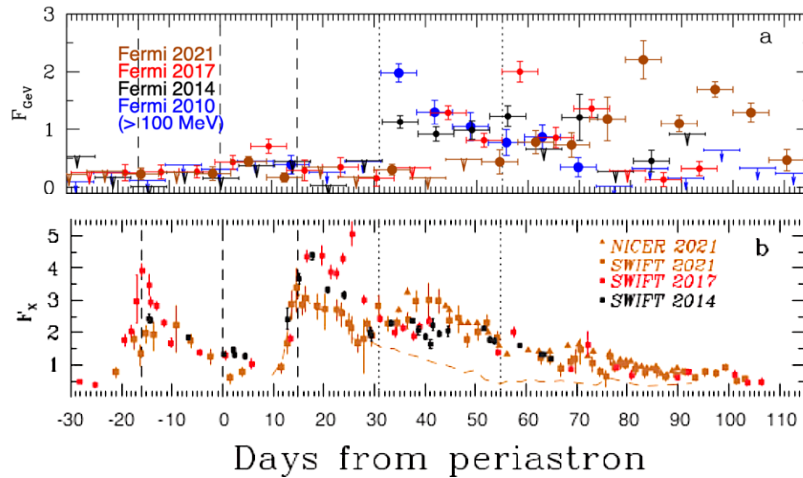


Figure 5: Evolution of PSR B1259-63 flux over the different periastron passages. Panel a: Fermi-LAT flux measurements in the $E > 100 \text{ MeV}$ range. Flux is given in $10^{-6} \text{ cm}^{-2} \text{ s}^{-1}$ and we observed the delay in the rise of the HE emission in the periastron

of 2021. Panel b: absorbed 1-10 keV X-ray flux in units of $10^{-11} \text{ erg cm}^{-2} \text{ s}^{-1}$, and we observe the unusual third peak only detected in 2021. Taken from [11].

LS 5039

It is one of the brightest gamma-ray binaries located in the Milky Way [13]. It is composed of a massive O star and a compact object, and it was first detected at VHE by H.E.S.S. [4] due to its location in the Southern Hemisphere. It has the shortest orbital period, which is about 3.9 days, of the so-far known gamma-ray binaries.

The HE gamma-ray emission occurs near the superior conjunction soon after the periastron passage, while the VHE emission is emitted around the inferior conjunction after the apastron passage [14]. This anti-correlation suggests a highly relativistic particle population that accounts for VHE emission mainly by synchrotron and anisotropic IC scattering of stellar photons, respectively. The HE gamma-ray peak would arise when TeV photons (of an IC origin) are absorbed through pair production as the NS approaches its O-type companion, and further enhances the HE emission through cascading effects [14]. This favors the pulsar-wind scenario for this binary, shown in Figure 2, but this proposal needs to be associated with the pulsar-stellar wind interaction. Recently, the short-term variability displayed in soft X-rays has been proposed to be caused by clumps of the companion star wind impacting the X-ray production site (see Figure 6). The observed timescale matches well with the lifetime of the clumps interacting with the pulsar wind and the dynamical timescale of the relativistic intrabinary shock in the pulsar wind scenario. [13].

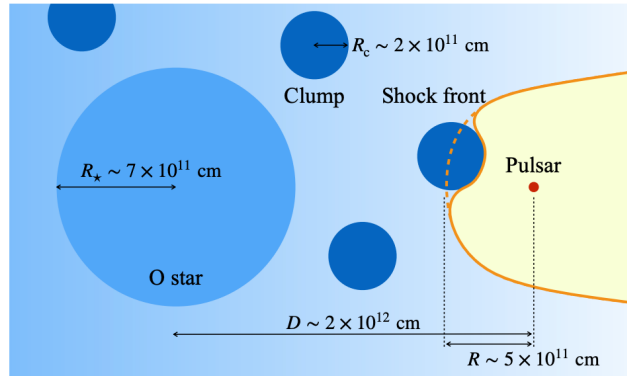


Figure 6: A schematic representation of the interaction of the stellar clumps with the pulsar winds. Taken from [13].

LS I+61°303

Located in the Northern Hemisphere, it was first detected at VHE by the MAGIC telescopes [5]. HE emission has also been reported by the gamma-ray satellite Fermi-LAT (Fermi-Large Area Telescope) [15]. It is composed of a Be star powered by a 0.27 s pulsar. These pulsations were recently discovered in radio by the FAST (Five-hundred-meter Aperture Spherical Telescope) radio telescope [16]. The identification of a pulsar powering the system reinforces the claims of magnetar-like flares (which is a NS with an extremely powerful magnetic field) from LS I+61303. If confirmed, this would be the first magnetar in a binary system [16].

HE gamma rays are emitted just after the periastron passage, while VHE gamma rays are detected during and just after the apastron [6]. The monitoring of this system shows that HE and VHE emissions are not correlated, which means that gamma-rays are originated

from different particle populations [14]. [17] proposed that these populations are produced by electrons accelerated on a double shock structure created within the binary system because of the interaction of the pulsar and massive star winds. The shock from the side of the pulsar can accelerate electrons to higher energies than the one from the side of the Be star. Thus, these two populations of electrons produce two-component gamma-ray spectra caused by the IC scattering of stellar radiation.

Besides the orbital period of 26.5 days, one of the unusual features of *LS I+61°303* is that the radio lightcurve displays periodic outbursts whose position and amplitude change from one orbit to the next, which has been associated with a super-orbital period of 1667 days related to the Be star disk [18]. MAGIC and VERITAS (Very Energetic Radiation Imaging Telescope Array System) observations spanning over two super-orbital periods [19] demonstrated that the TeV flux of the periodical outburst around apastron shows yearly variability consistent with the super-orbital period of 1667 days found in the radio band. Figure 7 displays this result.

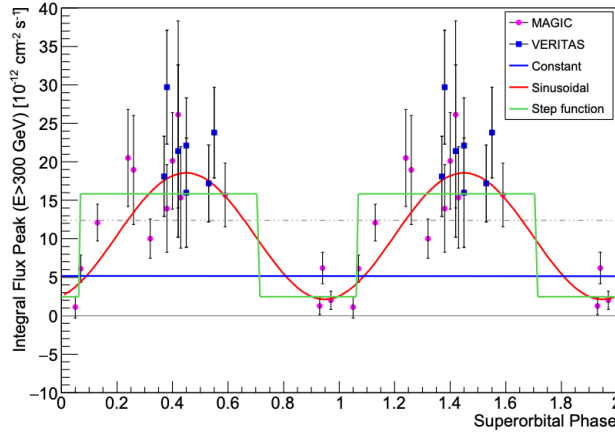


Figure 7: Integral flux peak of VHE emission in terms of the super-orbital period defined in radio. Taken from [19].

HESS J0632+057

This system was initially detected in VHE gamma rays as an unidentified point-like source by the H.E.S.S. experiment during observations of the Monoceros SNR (supernova remnant) [20]. *HESS J0632+057* is one of the faintest gamma-ray binaries. After observations in radio and X-ray, the binary nature was confirmed due to its spatial coincidence with the Be-type star MWC 148 and a compact object whose nature is still not known. The orbital period is about 316.7 days. The VHE emission corresponds to phases close to the apastron (see Figure 8). The VHE behavior of this source is very similar to that in *LS I +61°303* [6]. In contrast to other gamma-ray binaries, *HESS J0632+057* was the only system for a time undetected in the HE energy range. Only recently have reported HE gamma rays by Fermi-LAT after approximately 7.5 years of data [21].

A recent joint campaign with H.E.S.S., MAGIC and VERITAS confirmed, after accumulating more than 450 hours of data over 15 years, that the VHE orbital period is 316.7 days [22], allowing for the first time the determination of the period from VHE data, previously only measured in X-ray. The measured lightcurve has two peaks at VHE (see Figure 8).

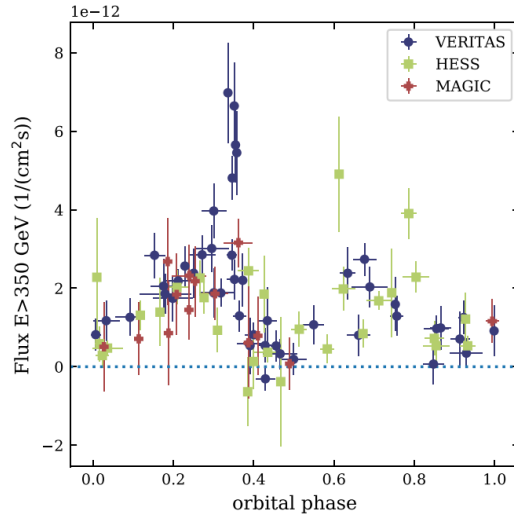


Figure 8: Gamma-ray lightcurve as a function of the orbital phase, assuming an orbital period of 317.3 days. VHE emission is detected by all the IACTs around 0.2, which correspond to apastron. Taken from [22]

The pulsar-wind scenario has been proposed for HESS J0632+057 [23, 24] due to similarities with other systems, although the microquasar scenario cannot be ruled out.

1FGL J1018.6-5856

This is the first gamma-ray binary system to be detected in the HE range through a blind search for periodic source in Fermi-LAT data [25]. It is composed of a massive O star and a compact object whose nature is still unknown. The system has an orbital period of 16.5 days.

Observations in the VHE range reveal two TeV sources (point-like *HESS J1018-589A* and *HESS J1018-589B*) within Fermi-LAT localization of *1FGL J1018.6-5856* [26]. The flux of *HESS J1018-589A* source was found to be variable on night-to-night basis and when convolved with the period detected in the HE range [26], so the binary *1FGL J1018.6-5856* correspond to *HESS J1018-589A*.

Based on optical spectroscopic observations, [27] found that the maxima of the X-ray, HE, and VHE flux correspond to the inferior conjunction. This finding was unexpected because gamma rays are believed to be produced through anisotropic IC up-scattering of the stellar UV photons. Therefore, the peak of the gamma-ray flux should occur at the superior conjunction. This discrepancy could only be explained if the binary orbit is eccentric and the flux maximum occurs at the periastron. These results were also verified with the comparison of the lightcurves in the X-ray and gamma-ray bands (see Figure 9) [14]. In addition, these spectroscopic observations of the optical counterpart [27] allowed to find that a companion star has a low radial velocity semi-amplitude of 11-12 km s⁻¹, which favors a NS as a compact object.

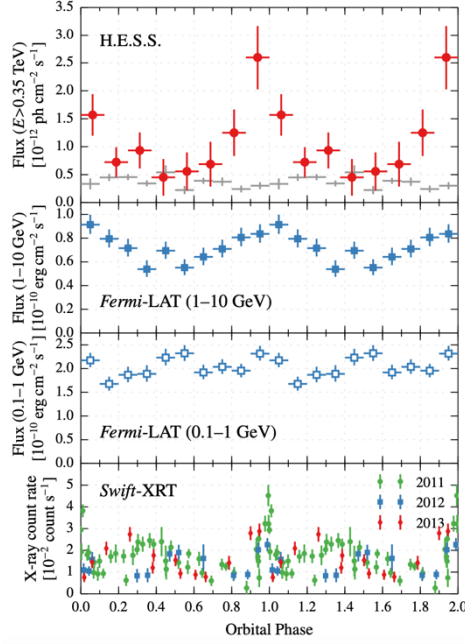


Figure 9: Lightcurves of 1FGL J1018.6-5856 which verified that the maxima of the X-ray, HE, and VHE flux correspond to the inferior conjunction. Taken from [26].

LMC-P3

It is the only gamma-ray binary detected outside the Milky Way, specifically in the Large Magellanic Cloud (LMC). It was discovered by Fermi-LAT [28], following the same blind search used for the discovery of 1FGL J1018.6-5856. LMC-P3 is composed of a massive O star inside SNR DEM L241. The nature of the compact object is still unknown, but the radial velocity measurements of the O star and the source properties suggest that it is a rapidly rotating neutron star [28]. The HE emission occurs near the superior conjunction, while VHE emission occurs in the inferior conjunction [29]. The orbital period is about 10.3 days [28]. This binary system presents strong similarities to LS 5039 and 1FGL J1018.6-5856, but it is significantly brighter in HE gamma-ray emission, radio, and X-ray [14].

PSR J2032+4127

It is a binary system formed by a 143ms pulsar orbiting the Be-type star MT91 213. The pulsar was first detected in radio by Fermi-LAT [30], and after some years of analysis of both gamma-ray and radio timing data, they showed in 2017 that the projected position of the pulsar lay close to MT91 213 [31]. Thus, PSR J2032+4127 is the second gamma-ray binary in which the nature of the compact object is clearly established.

The periastron passage of 2017 allowed MAGIC and VERITAS [32] to study the properties of the system. Both VHE and HE emission took place during periastron passage, with VHE emission showing strong daily variability [32]. In addition, the orbital period of the system is about 50 years, so it is the gamma-ray binary with the largest period. Besides, particles are accelerated at the shock that forms between the pulsar and Be star winds. These subsequently produce synchrotron emission from radio to X-ray bands and inverse Compton emission at VHE gamma rays [32].

We study more deeply PSR J2032+4127 in Chapter 7 of this work, to analyze the high-level MAGIC data of this source and compare it to [32]. Furthermore, the pulsar of this binary remains a plausible candidate for the power source driving TeV J2032+4130 [32],

a steady VHE nebula that contributes as background noise in the results obtained for this binary in the VHE gamma-ray range.

HESS J1832-093

It has been a gamma-ray candidate discovered as a TeV point by H.E.S.S. [33]. This source lies in the vicinity of SNR G22.7-0.2, which can suggest its possible association with this SNR.

Recently, a study of this TeV source has been performed with Fermi-LAT and Swift data [34], in which mainly the obtention of an orbital period of approximately 86 days and a SED similar to that of HESS J0632+057 allow the identification of HESS J1832-093 as a new gamma-ray binary [34]. Future multi-wavelength observations will be able to establish the properties of this binary.

Most gamma-ray binaries, as mentioned earlier, show similar characteristics in their radio and X-ray emissions. However, considering the main features of the so-far known gamma-ray binaries, a few open questions about this sub-class of gamma-loud binaries are:

- Powering engine: only in the case of PSR B1259-63, LS I +61°303 and PSR J2032+4127, a pulsar has been firmly identified as the compact object. In the rest of the gamma-ray binaries, both the pulsar-wind scenario and the microquasar scenario must be considered. However, due to similarities between systems, it is possible that most gamma-ray binaries host a pulsar.
- Lightcurve profiles: Lightcurves in the few gamma-ray binaries known so far display in most cases distinct features. These include asymmetric profiles in the lightcurve of *PSR B1259-63*; non-negligible fluxes at orbital phases where absorption should be severe in *LS 5039*; sharp dips and double-peak profiles in *HESS J0632+057*; cycle-to-cycle variability of the main VHE peak in *LS I +61 303* [8]. The existence of differences between lightcurves of the same gamma-loud binary sub-class needs to be investigated.
- SEDs: while the VHE of most gamma-ray binaries can be modeled as power laws, some cases present energy cutoffs, such as the case of the high-state in *HESS J0632+057* or possibly *PSR J2032+4127* during periastron. To account for this difference, either deeper observations or more sensitive instruments would be needed.

5. Gamma-ray emitting binaries

Las binarias emisoras de rayos gamma son aquellas que no emiten la mayor parte de su radiación no térmica en el régimen de rayos gamma, sino a energías menores. En esta categoría de binarias brillantes en gamma se incluyen microcuásares, binarias de viento en colisión y novas. En este capítulo se muestran las principales características de cada sistema y cuestiones que han quedado sin resolver.

Gamma-ray emitting binaries are those systems that do not emit the bulk of their non-thermal radiation in the gamma-ray regime, but at lower energies. In Figure 10, we show an example of the SED of the microquasar Cygnus X-1.

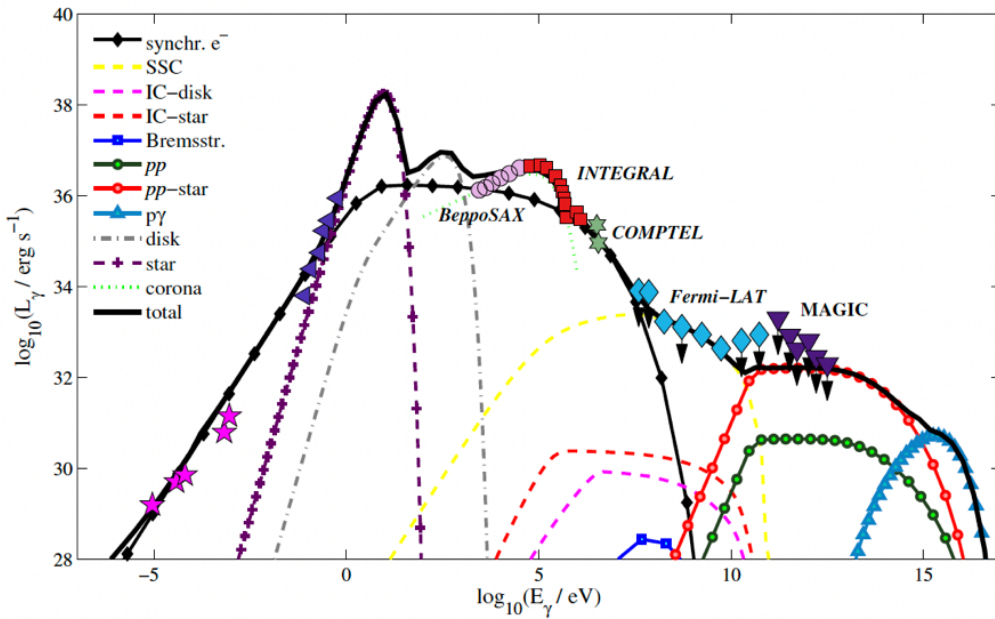


Figure 10: Best-fit SED for the microquasar Cygnus X-1. The X-ray emission takes place approximately in $\log(5)$, and the gamma-ray band is above $\log(8)$. This is an example of a typical SED for gamma-ray emitting binaries. Taken from [35].

This new category was needed after the discovery at HE and/or VHE of different types of systems, which were found to emit gamma rays with different characteristics to traditional gamma-ray binaries and that were composed of different bodies. In this gamma-loud binaries sub-class, microquasars, colliding wind binaries (CWB), and novae are included. Table 2 shows the main characteristics of the gamma-ray emitting binaries studied in this work. In the subsections of this chapter, we dive into each binary.

<i>Gamma-ray emitting binary</i>	<i>Type</i>	<i>Star Type</i>	<i>Compact Object or companion star</i>	<i>Distance [kpc]</i>	<i>P_{orb}</i>	<i>HE γ-ray emission</i>	<i>VHE γ-ray emission</i>
Cygnus X-1	Microquasar	O supergiant star	BH	1.9	5.6 d	yes	-
Cygnus X-3	Microquasar	Wolf-Rayet star	-	7.2	4.8 h	yes	-
SS 433	Microquasar	Supergiant star	-	\sim 5	\sim 13 d	yes	yes
V4641 Sgr	Microquasar	B giant	BH	0.5	2.8 d	-	yes?
Eta Carinae	CWB	LBV star	O or Wolf-Rayet	2.3	5.5 yrs	yes	yes
RS Ophiuchi	Nova	Red giant	White dwarf	\sim 4.5	\sim 1.2 yrs	yes	yes

Table 1: Parameters of some gamma-ray emitting binaries. From left to right, the quoted parameters are the gamma-ray emitting binary, the type of gamma-ray emitting binary, its star type, its compact object or companion star, the distance between the system and The Earth [in kpc], the orbital period of the binary system, and the detection of HE/VHE γ -ray emissions.

5.1. Microquasars

Microquasars are binary systems powered by accretion onto a black hole or a neutron star that display relativistic jets [8], as explained in the introduction. The particle energy in microquasar jets is comparable with that in Active Galactic Nuclei (AGN), which is a compact region at the center of a galaxy that presents non-stellar radiation, so the compact region has been related to a supermassive BH. Blazars are AGNs whose jets are pointing at the observer. Thus, it is expected that microquasars whose jets are pointing to the Earth appear as scale-down versions of blazars, which have been named microblazars [7].

The main feature of microquasars is that they display distinct X-ray spectral states, which are the result of variable accretion rates onto the compact object. During the hard state, microquasars display transient relativistic jets, that disappear during the low state and quiescence. Persistent jets have been found in a few systems. These jets can potentially produce gamma rays [8].

The so-far known microquasars detected in HE and/or VHE gamma rays are:

Cygnus X-1

This system is a binary composed of a $14.8 M_{\odot}$ BH on an almost circular 5.6 days orbit around a $19.2 M_{\odot}$ O supergiant star [36]. The orbital period was detected by radio and X-ray observations [37]. *Cygnus X-1* was classified as microquasar after the detection of a one-side relativistic radio-jet [38]. It displayed the two principal X-ray states of BH

transient, the soft state and the hard state. During the hard state the source displays persistent jets from which synchrotron radio emission is detected, while in the soft state, these jets are disrupted.

Analysis of more than 7 years of Fermi-LAT data allowed for the discovery of HE gamma-ray emission from *Cygnus-X1* [39] during hard state. This emission has been related to IC scattering mechanism. MAGIC observations of this source displayed a 4σ hint of emission at VHE in an 80-minutes observation coincident with a hard X-ray flare [40]. No persistent VHE emission has been detected [41].

Cygnus X-3

It is the only known binary in the Galaxy containing both a compact object and a Wolf-Rayet star with a very short orbital period of 4.8h [14]. The compactness of the system produces an unusually high absorption, probably caused by the wind of the companion star, which complicates the identification of the compact object ($1.4M_{\odot}$ NS, or less than $10M_{\odot}$ BH). Despite this strong X-ray absorption, the X-ray spectrum shows two main spectral X-ray states resembling the states of BH transient. This allows to consider it a microquasar.

HE gamma-ray emission was discovered by Fermi-LAT and AGILE (Astrorivelatore Gamma ad Imagini Leggero) [42, 43] in the soft spectral state, displayed as transient emission which has been related to IC scattering mechanism.

VHE emission was not found by MAGIC [44]. The extremely high absorption due to the Wolf-Rayet could affect VHE gamma-ray emission.

SS 433

This binary system is composed of a supergiant star that is overflowing its Roche Lobe with matter accreting onto a compact object which is most likely a BH [45]. Two jets of ionized matter extend from the binary, perpendicular to the line of sight, and terminate inside the SNR *W50* [43]. The detection of the jets supposed the identification of this source as a microquasar. The lobes of *W50* in which the jets terminate, about 40 parsec of the central source, are accelerating charged particles consistent with electron synchrotron emission according to radio and X-ray observations [46]. Figure 11 displays a representation of *SS 433*.

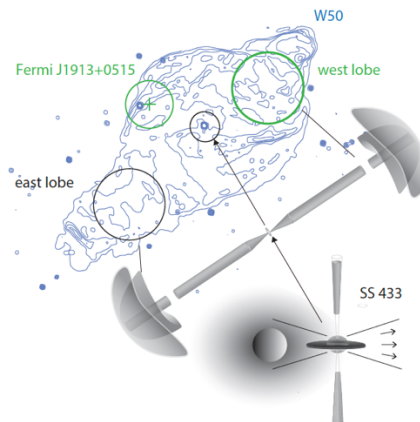


Figure 11: representation of SS 433/W50. The circles indicate the regions in which HE (Fermi) and VHE (west lobe and east lobe) gamma rays are emitted. Credit: P. Bordas.

The High Altitude Water Cherenkov (HAWC) Observatory detected VHE gamma rays from *SS 433* and suggest that the highly energetic electrons in the microquasar are probably accelerated in the jets and near the VHE gamma-ray emission regions, which are the eastern (e_1) and western (w_1) interaction regions of the jets with *W50* [47]. According to the observed flux, protons as the primary particles of the VHE gamma rays are an unlikely scenario because the total energy required to produce the highly relativistic protons is too high, and the jets of *SS 433* are known to be radiatively inefficient. This is the first time that VHE emission has been detected from a microquasar. After several years of search by IACTs [48], H.E.S.S. confirmed the detection of TeV emission in the jet-nebula interaction regions [49].

Several publications report the detection of *SS 433* at HE with Fermi-LAT data. However, the region is complex to analyze and there is strong contamination from nearby sources. Recently, [50] reported the detection of HE emission in the nebula, not coincident with the HAWC emission but showing the same periodicity as the jet precession.

V4641 Sgr

It is one of the three microblazar candidates in the Milky Way. It is composed of a late B-type giant of about $3M_{\odot}$ and a BH of about $6M_{\odot}$. The orbital period is 2.8 days. It has recently been reported as a new TeV source by HAWC [51]. If the extended emission reported by HAWC is indeed connected to *V4641 Sgr*, this would be the first gamma-ray emitting microblazar.

The production of gamma-rays in microquasars can have theoretically a leptonic origin, in which IC scattering takes place, or a hadronic origin, in which the pion (π^0) decay is the mechanism of production. Considering this and the previous features of the microquasars detected at VHE and/or HE, the open questions for this type of gamma-loud binaries are [8]:

- A small population: only a few microquasar has been reported as gamma-ray emitters. Only steady emission from the microquasar *SS 433* has been detected at VHE, while no transient emission has ever been reported. On the other hand, *V4641 Sgr* has not been detected at HE. Thus, it is important to study the microquasars limitation in producing detectable levels of gamma rays in certain ranges, for which a deeper knowledge of the physic behind state transitions is necessary. It is expected though that with more sensitive telescopes such as CTA (Cherenkov Telescope Array), transient and persistent emission from microquasars such as Cygnus X-1 and Xygnus X-3 is detected [52].
- Jet physics: understanding the conversion of accretion or BH rotation into powerful kinetic ejections, the jet composition, and the acceleration process, are the clue for achieving a deeper knowledge about microquasars.
- Contribution to Galactic cosmic rays: cosmic rays are mainly the protons that permeate the Milky Way. In the hadronic context theoretically proposed, microquasars could be contributors to the Galactic cosmic-ray sea.

5.2. Colliding wind binaries (CWB)

Contrary to all other gamma-loud binaries, colliding wind binaries are not composed of a compact object. These systems are formed by two massive stars, and gamma rays can be produced in the shock interface of the two star winds [8]. Only one

CWB has been firmly detected in gamma rays: Eta Carinae. Hints of HE gamma-ray emission in γ^2 Velorum has been recently detected [53] during the apastron, but deeper studies are needed to know the properties of this CWB. Thus, we focus on Eta Carinae.

Eta Carinae is composed of a primary Luminous Blue Variable (LBV) with a mass greater than 80 solar masses. Its companion has not been directly observed but inferred from its orbital variability to be an O or Wolf-Rayet star with 30-50 solar masses [54]. It is in the Carina arm at a distance of ~ 2350 pc. This CWB emits hard X-rays, and the gamma-ray emission is modulated by the orbital period of approximately 5.5 years. Gamma-ray emission was first detected by AGILE [55] in the periastron passage. Its spectrum has been widely studied above 100 MeV, where two distinct components are detected above (High-Energy:HE) and below (Low-Energy: LE) 10 GeV [54]. Despite the HE component has a hadronic origin, at LE both leptonic and hadronic scenarios are still plausible. Recently, VHE gamma rays produced in a leptonic scenario have also been detected by H.E.S.S. [56] before and after the minimum in the X-ray lightcurve close to the periastron. In addition, recent gamma-ray observations of Eta Carinae strongly suggest that the wind collision region is perturbed orbit to orbit affecting particle transport within the shock [54].

Considering that only Eta Carinae has been firmly detected at gamma-ray energies, the open question related to CWB is why this sub-class of gamma-loud binaries present such a small population. Future studies related to γ^2 Velorum and a reanalysis of the Fermi-LAT data set could enhance the number of CWB detected.

5.3. *Novae*

Novae are optically variable binary systems with a mass transfer from a companion star to a white dwarf, resulting in thermonuclear explosions on the surface of the white dwarf. Nova outbursts usually last from weeks to months. While they are expected to repeat hundreds of times, the interval between consecutive thermonuclear explosions can be as long as hundreds of thousands of years.

Two sub-class of novae can be defined: the classical nova, in which the white dwarf accretes material from the Roche-Lobe overflow of the low-mass companion star, and the symbiotic nova, which is formed when the companion star of the white dwarf is a red giant (RG). The ejecta of symbiotic novae expands within the dense wind of the RG companion. In addition, if the outburst of symbiotic nova occurs repeatedly over a human lifespan, it is named recurrent symbiotic nova.

The first nova to be detected at HE gamma rays was the symbiotic nova V407 Cyg [57]. Fermi-LAT also discovered that classical novae are HE emitters [58]. During the last decade, a large number of novae have been detected by Fermi-LAT at HE¹. In this work, we focus on RS Ophiuchi, the first nova to be detected at VHE gamma rays [59].

¹ For a full list of Fermi-LAT detected novae check:
<https://asd.gsfc.nasa.gov/Koji.Mukai/novae/latnovae.html>

RS Ophiuchi is a recurrent symbiotic nova that has an average time between major outbursts of 14.7 years. Recently, the explosion of this nova was first reported at HE gamma rays by Fermi-LAT [60]. Later, it was detected at VHE by H.E.S.S. [61], MAGIC [59], and the prototype Large Size Telescope (LST1) [62] of CTA. Figure 12 shows the SED obtained by MAGIC during the first 4 nights of observations, spanning from 60 GeV to 250 GeV [59]. It allowed to conclude that π^0 - decay is the mechanism of production of gamma rays. These protons accelerated by the nova can create local bubbled of enhanced cosmic-ray emission, which has helped in understanding the contribution of novae to the bulk of Galactic cosmic rays.

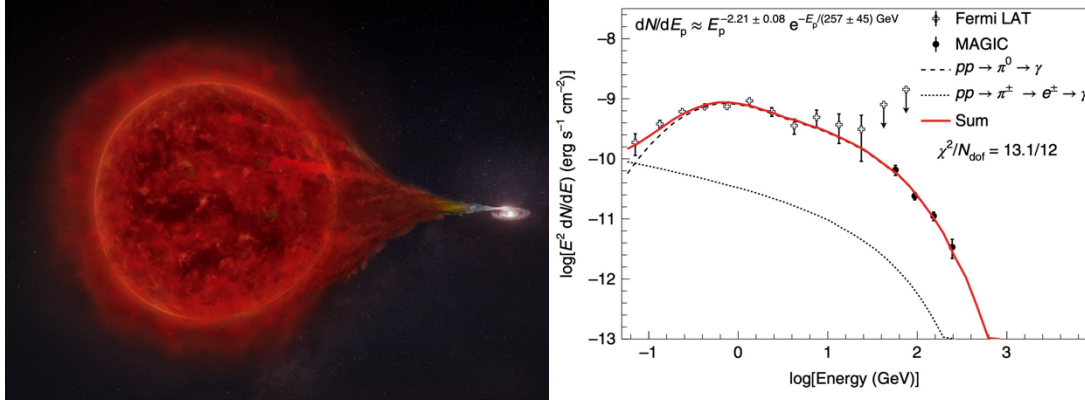


Figure 12: Left: illustration of RS Ophiuchi (image credit²) Right: the hadronic model obtained during the first 4 nights of observations, taken from [59].

Over the years, an open question related to novae is why none of them had been detected at VHE [8]. With the discovery of RS Ophiuchi as the first VHE gamma-ray emitting nova, the possibility to detect this emission from other novae has opened a new window in VHE astronomy.

² <https://superbossa.com/MPP>

6. The MAGIC telescopes and introduction to data analysis.

MAGIC son dos telescopios Cherenkov situados en el Observatorio del Roque de los Muchachos (La Palma) que detectan rayos gamma desde 50 GeV hasta 100 TeV. En este capítulo se detallan las características principales de estos telescopios. También se introducen los diferentes niveles de reconstrucción de datos que permiten evaluar la señal observada, obtener la forma y la localización de la fuente de rayos gamma y confirmar su detección a muy altas energías.

The MAGIC telescopes are IACTs which are located on the Roque de los Muchachos Observatory on the Canary Island of La Palma. The scientific observations with the first MAGIC telescope, MAGIC-I, began in 2004 and the second telescope, MAGIC-II, has been operational since 2009 [63]. They operate jointly in stereoscopic mode.



Figure 13: Picture of the MAGIC telescopes. Credit: G. Ceribella

The MAGIC telescopes are dedicated to the observation of gamma rays from galactic and extragalactic sources in the VHE range, from ~ 50 GeV to 100 TeV [63]. The gamma rays are indirectly detected via the Cherenkov effect. The primary gamma ray interacts with the molecules of the upper atmosphere producing an electron-positron pair. Both particles decay into a photon, and each photon again produces an electron-positron pair. This reaction takes place several times forming the so-called electromagnetic shower. These charged particles move faster than the speed of light in the atmosphere, radiating low-energy (blue to ultraviolet) photons, which constitute the Cherenkov radiation observed by the IACTs. This radiation is emitted in a cone and has an energy that can be used to infer the energy of the primary gamma ray. It is worth noticing that cosmic rays (protons and light-ionized atoms) can also generate hadronic showers that develop differently in the atmosphere but also radiate Cherenkov photons, creating a source of background.

The Cherenkov radiation produced by gamma rays can be marginally detectable due to the low proportion of gamma rays that achieve to interact with the atmosphere. Gamma

rays are less numerous than protons or light-ionized atoms, which are the particles that mostly compose the cosmic-ray background. The detection of such a weak signal requires high instrumental sensitivity and large collection areas. In the case of the MAGIC telescopes, the main characteristics that maximized the sensitivity are [63]:

- A large collection area with an active mirror surface of 236 m² and a diameter of 17 m.
- MAGIC-I and MAGIC-II are separated by 85 meters and, to increase the sensitivity, they are usually operated in coincidence, in the so-called stereoscopic mode.
- The two telescopes are located at a height of 2200 meters at sea level, in mountains so far from the background light, with a clear atmosphere.
- Both telescopes have an approximately hexagonal camera of 1.05 m diameter, with 1039 photomultiplier tubes (PMTs). Each PMT acts like a pixel, covering 0.1°. PMTs are used not only for maximizing sensitivity but also for achieving a fast detection of the Cherenkov flashes. In addition, PMTs have a peak efficiency of approximately 32% and allow observations under moderate moonlight conditions without damaging the camera.
- The maximum repositioning speed is more than 7 degrees per second, meaning the telescopes can be pointed to any point on the observable sky in less than 25 seconds due to a weight of only around 60 tons, optimized for detecting transient events.

The previous characteristics allow the observation of the Cherenkov photons produced by gamma rays from a galactic or extragalactic source. Once a hint of this type of signal is collected with the MAGIC telescopes, the data analysis aims to confirm the detection of a source at very high energies, obtain the location and the shape of the source, and evaluate the signal obtained.

The software used for data analysis is MARS, an acronym for MAGIC Analysis and Reconstruction Software [64]. MARS is written in C++ programming language and operates in a ROOT environment [65].

The main steps of the MARS routines used in the data reconstruction and evaluation are³:

- Low-level data reconstruction: consist of signal extraction. Each telescope's data are treated separately to perform the image cleaning, using the information from the pixels to identify which ones belong to the Cherenkov shower and which ones correspond to the background noise. Also, an arrival time is assigned to each pixel for improving the Cherenkov shower and background noise pixel selection. See Figure 14 for an example of image cleaning in MAGIC.

³ See i.e. [66] for a detailed explanation of each step.

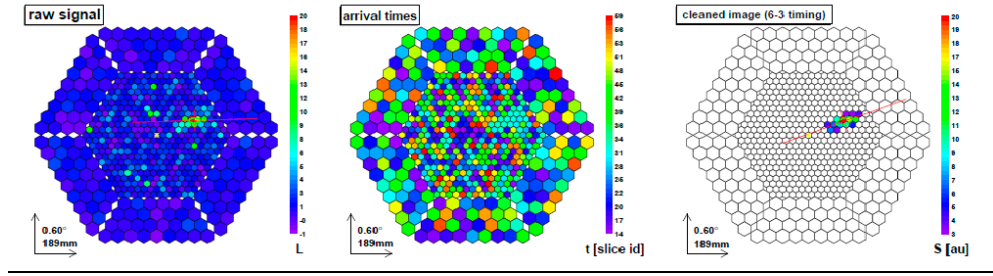


Figure 14: Image cleaning method. From left to right, the raw signal, the arrival times, and the cleaned image. The last one corresponds to an electromagnetic shower due to its compact and elliptical shape. Taken from [67].

- Intermediate-level data reconstruction: consist of event reconstruction, background discrimination, and energy estimation. Once the image cleaning is done, individual telescope files contain information about the Hillas parameters for each event, which allow parametrizing the image, modeled as an ellipse. The Hillas parameter that is mentioned in this work is θ , which is the angular distance between the position of the source and the estimated source position for an event. In the analysis, θ^2 is more commonly used, since the background distribution is approximately flat while the gamma-ray distribution is exponential. After this procedure, the executable Melibea allows the discrimination between gamma rays and the hadronic background and estimates the energy and incoming direction of the primary event.
- High-level data reconstruction: consist of the signal evaluation, extracting the skymap, energy spectrum, and lightcurve of the source once the data files have been correctly produced. The MARS routines for this high-level analysis are Odie (signal evaluation), Caspar (skymap), and Flute (SED and lightcurve).

In this work, we use a subsample of the published data from the binary *PSR J2032+4127* to get acquainted with the MAGIC high-level data analysis. These data were obtained in November 2017, during the periastron passage, accumulating a total of about 8 h of good quality data.

7. Data analysis, results and discussion

Este capítulo consta de dos apartados. El primero consiste en el análisis de datos de alto nivel de la binaria de rayos gamma PSR J2032+4127, en el que analizamos 8.21 horas de datos de buena calidad para realizar la evaluación de la señal, obtener el mapa del cielo y calcular la distribución de energía espectral y la curva de luz. Estos resultados se comparan con los publicados en [32]. El segundo apartado consiste en evaluar si la candidata a binaria de rayos gamma HESS J1828-099 podría ser detectada con los telescopios MAGIC. Las distribuciones de energía espectral simuladas nos permiten discutir cuántas horas de exposición son necesarias para detectar esa binaria si quisiéramos elaborar una propuesta de observación.

7.1. Data analysis of the gamma-ray binary PSR J2032+4127

In this section, we focus on the high-level data reconstruction of the binary PSR J2032+4127. We perform the signal evaluation, obtain the skymap and calculate the SED and lightcurve making use of different MARS routines⁴. We analyze 8.21 hours of good quality data, and the results are compared with those obtained in [32].

7.1.1. Signal evaluation

The routine Odie allows the user to evaluate the On and Off event distribution with the Hillas parameter θ^2 by generating $N_{on} - \theta^2$ and $N_{off} - \theta^2$ histograms, where N_{on} and N_{off} are the number of signal and background events in the defined region respectively. Odie also analyzes the number of gamma-ray excess events, $N_{ex} = N_{on} - N_{off}$, with θ^2 . The signal is determined by all the excess events within an upper θ^2 cut, while the background flux follows a flat distribution with θ^2 . Odie also performs an estimation of the source extension and the Point Spread Function (PSF) by fitting the N_{ex} histogram.

The other important characteristic of this routine is the calculation of the significance. The significance is defined by the Li & Ma formula [68], given by Equation (1),

$$\sigma = \sqrt{2} \left\{ N_{on} \log \left[(\tau + 1) \left(\frac{N_{on}}{N_{on} + N_{off}} \right) \right] + N_{off} \log \left[\left(\frac{1 + \tau}{\tau} \right) \left(\frac{N_{off}}{N_{on} + N_{off}} \right) \right] \right\}^{\frac{1}{2}} \quad (1)$$

where τ is the ratio of Off to On exposure.

In the data analysis of the gamma-ray binary PSR J2032+4127, Odie was used for determining the number of events with θ^2 . We use the standard θ^2 cuts, which take into account the current telescope configuration. In addition, the PSF can be defined as a 2D -gaussian with a sigma equal to psf40, which is a fixed parameter related to the

⁴ In this work, the MARS routines Odie, Caspar, and Flute are explained following the reference [66].

The significance, obtained with the Equation (1), at low energies is 6.6σ , in full range is 7.3σ , and at high energies is 3.1σ . Thus, we can confirm the detection of *PSR J2032+4127* at low energies and in full range, with a hint of signal at 1 TeV. Probably increasing the observation time would lead to the detection at high energies.

Moreover, the plots at low energies and in full range show an approximately flat distribution, although we can expect some contamination from the nebula *TeV J2032+4130*. In the publication [32], this background noise is separated from the gamma rays produced in the binary, which is not the objective of this work, since it would require a much more complex analysis. However, our signal evaluation is compatible with the obtained in [32].

7.1.2. *Skymap*

The routine Caspar generates the skymap by transforming the reconstructed arrival direction into events in the sky, obtaining a random distribution around the true position of the source, that corresponds to the PSF.

The standard cuts are also used in the routine Caspar. The skymap of the gamma-ray binary *PSR J2032+4127* is obtained at low energies, full range, and high energies (see Figure 16):

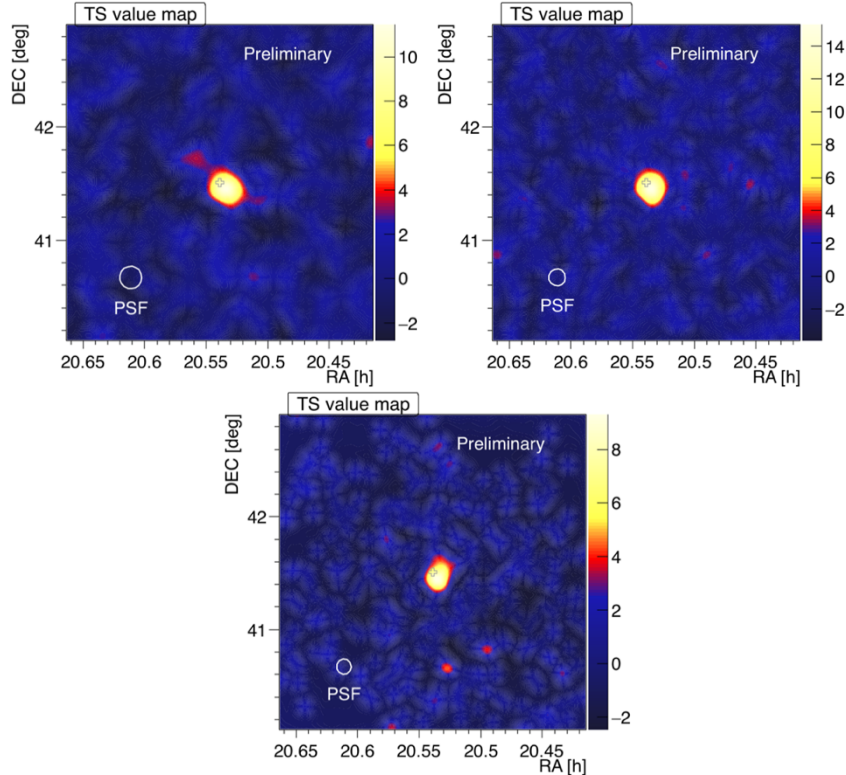


Figure 16: *Skymaps of PSR J2032+4127. Top left: Skymap at low energies; Top right: Skymap in full range; Bottom: Skymap at high energies. The data was obtained after 8.21 hours of observation.*

Each obtained skymap of *PSR J2032+4127* has a maximum value of significance. The skymap at low energies shows a maximum significance value of approximately 11σ , in the full range this value is around 15σ , and the skymap has significance of approximately 8σ at high energies. Thus, *PSR J2032+4127* has been detected with the evaluation of the skymaps in the different energy ranges.

However, the routine Odie shows a significance value of 3.1σ at high energies (see Figure 15), so the gamma-ray binary is detected with the routine Caspar but not with Odie at energies higher than 1 TeV. The fact that these routines have different forms to evaluate the background noise explains the different significance obtained.

Besides, the skymap presents a background noise due to the nebula *TeV J2032+4130*. In the skymap of [32], a more advanced analysis method was used to separate the background noise of the gamma-ray events produced in the binary *PSR J2032+4127*, which was not the objective of this work.

7.1.3. Spectral energy distribution (SED) and lightcurve

The spectral energy distribution (SED), the flux, and the lightcurve (the flux evolution with time) can be obtained with the routine Flute. The flux is defined as the rate of gamma rays per area unit as follows:

$$\Phi = \frac{d^2N}{dSdt} \text{ cm}^{-2}\text{s}^{-1} \quad (2)$$

Where N is the number of detected gamma rays, calculated as $N = N_{on} - N_{off}$, dt represents the effective observation time and S is the effective collection area, calculated from Monte Carlo (MC) simulated events.

The SED, which represents the energy flux per interval of energy, can be calculated as:

$$E^2 \frac{d\Phi}{dE} \text{ TeV cm}^{-2}\text{s}^{-1} \quad (3)$$

Another important concept derived from the definition of the flux is the integral flux, which is the total flux in an energy range above an energy value E_{low} , given by Equation (4):

$$\Phi_{E>E_{low} \text{ GeV}} = \int_{E_{low}}^{\infty} \frac{d\Phi}{dE} dE \text{ cm}^{-2}\text{s}^{-1} \quad (4)$$

With the integral flux, we can define the lightcurve as the evolution of the integral flux over time in a certain energy range.

SED

The SED is obtained with the executable Flute by defining the right ascension and declination of the source. Also, we must define the minimum and maximum values between 10 and 60 degrees for the Zenith respectively, which is important for the MC simulated events. Also, a default background estimation mode is used. The number of bins or range to estimate the energy can be modified according to the obtained data. For the binary *PSR J2032+4127*, after testing different numbers of bins, the selected number is 20 bins.

The SED related to the gamma-ray binary *PSR J2032+4127* was obtained assuming a spectral shape that follows the power law $(\frac{x}{b})^\Gamma$. That power law is normalized to $b = 200$ GeV and the assumed spectral index is $\Gamma = -2.6$, a typical value for the gamma-ray binaries [8]. The SED and the representation of the number of detected gamma rays in an estimated range of energy are shown in Figure 17 and Figure 18 respectively:

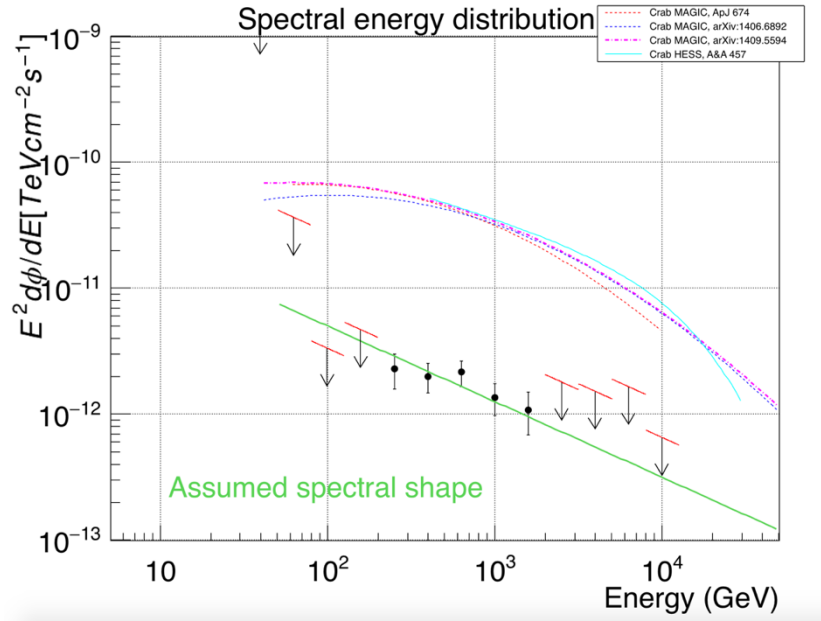


Figure 17: SED of the gamma-ray binary *PSR J2032+4127*. The spectrum of the Crab Nebula is plotted as a reference.

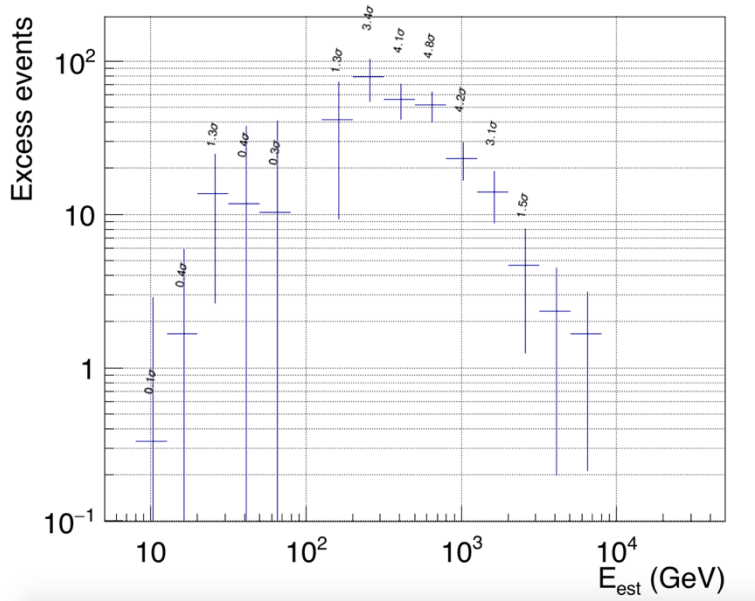


Figure 18: Representation of the excess gamma-ray events detected in the binary PSR J2032+4127 as a function of the estimated energy in units of GeV. With the executable *Flute*, the detected events have a significance higher than 2σ .

The representation of Figure 18 shows detected gamma-ray events between 200 GeV and 1 TeV approximately, which is the same range of energy in which the points in the SED are represented (the other points are upper limits, which correspond to the events that have not been detected, with a significance lower than 2σ).

In the publication [32], a more complex analysis is performed for extracting the SED, considering that there is a background source, the nebula *TeV J2032+4130*. Since that corresponds to an expert-level analysis, it goes beyond the scope of this work. However, our results fit the PWL shape also obtained in the publication.

The resulting SED is obtained for an estimated value of energy. However, we can obtain the SED for a true value of energy using the *Fold* program. *Fold* considers that the detection of a source suffers from several issues like limited acceptance since not all the gamma rays entering the atmosphere are detected by the telescope. The energy estimation has a limited resolution of around a 15% in the case of the *MAGIC* telescopes. Thus, the executable *Fold* solves these problems via forward-folding Poissonian Likelihood maximization, transforming the distribution of an observable (E_{est}) into a true distribution of a physical quantity (E_{true}). In this case, the obtained SED of *PSR J2032+4127* is shown in Figure 19.

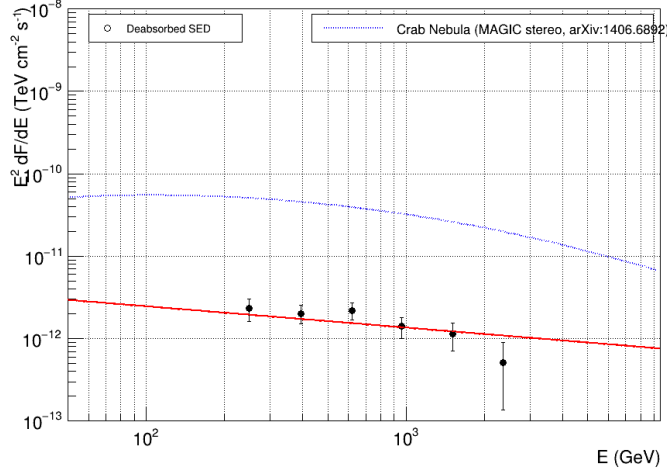


Figure 19: SED of PSR J2032+4127 for a true value of energy. The spectrum of Crab Nebula is included as a reference.

The SED of Figure 19 shows five points corresponding to detected gamma-ray events between 200 GeV and 1 TeV approximately (the point above 2 TeV is an upper limit). The results of assuming a spectral shape that follows the power law $\alpha(\frac{x}{b})^\Gamma$ are: the integral flux, α , is $\alpha = (5.13 \pm 1.02) \cdot 10^{-11} \text{ cm}^{-2} \text{ s}^{-1}$, b is the pivot energy of 200 GeV, and the spectral index is $\Gamma = -2.26 \pm 0.13$. These values are compatible with those published in [32] within statistical uncertainties.

Lightcurve

We are interested in understanding the evolution of the gamma-ray flux with time. The routine Flute allows the calculation of the flux per day or in a user-defined bin, in which the integral flux is obtained. In Figure 20, we can see the calculated daily lightcurve (in Modified Julian Days, MJD) and the average integral flux.

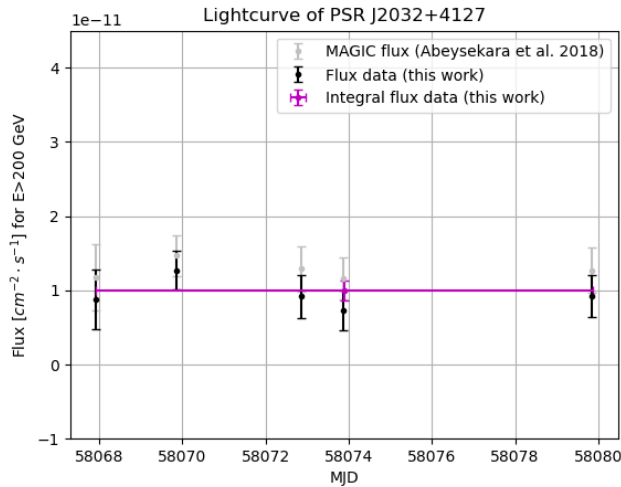


Figure 20: Lightcurve of PSR J2032+4127. Python was used to represent the flux data (in black), and the integral flux (in magenta), both obtained with the executable Flute in this work. The flux data represented in grey correspond to those published in [32].

The lightcurve of *PSR J2032+4127* shows that the fluxes obtained in this work are compatible with those published in [32] within statistical uncertainties. The obtained value for the integral flux at energies above 200 GeV is $(9.96 \pm 1.37) \cdot 10^{-12} \text{ cm}^{-2} \text{ s}^{-1}$.

7.2. Evaluation of the gamma-ray binary candidate *HESS J1828-099* for MAGIC observations.

HESS J1828-099 is a source whose nature is still unknown. It was discovered during the H.E.S.S. Galactic Plane Survey [69]. [70] recently suggested that this source could be a new TeV gamma-ray binary system.

In this work, we aim at studying how much time of observation would be needed to detect with high significance this source with MAGIC to understand the nature of this source with a hypothetical observational proposal. For this purpose, we use the script MAGIC Source Simulator (MSS) provided by the MAGIC collaboration. The executable takes a given spectral shape and uses the MAGIC performance [63] in the range from 40 GeV to 16 TeV. The obtained SED shows the significance of each spectral point, which is calculated according to the Li and Ma formula [68] (see Equation 1).

To obtain that estimation of the SED for *HESS J1828-099* with the MSS, a simple power law is used, in which the pivot energy is 1400 GeV, the differential flux at the pivot energy is $2.24 \cdot 10^{-13} \text{ cm}^{-2} \text{ s}^{-1} \text{ TeV}^{-1}$, and the spectral index is -2.25. These values are obtained from the measured SED from H.E.S.S. [69].

In this case, the expected MAGIC spectral energy distribution was obtained for 30, 60, and 80 hours of observation, as Figure 21 shows.

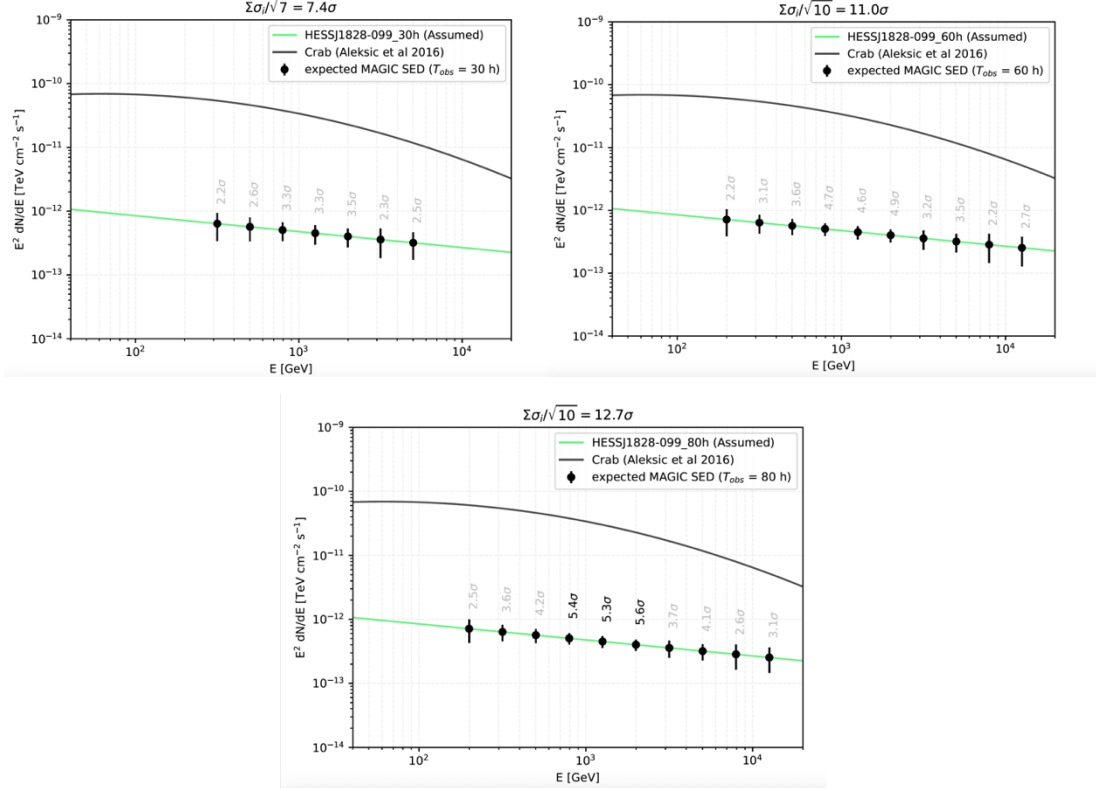


Figure 21: Expected MAGIC SEDs of HESS J1828-099. Top left: SED after 30 hours of observations; Top right: SED after 60 hours of observation; Bottom: SED after 80 hours of observations.

In the case of SED, we consider a flux point whenever its significance is higher than 2σ . Also, for a good SED, we need to have a large number of points. In Figure 19, all spectral points have a value of significance higher than 2σ . We can see that already with 30 hours of observations, we would be able to extract a nice SED and that we would detect the source with an overall significance of about 7.4σ . However, since we aim at studying the nature of the source with higher statistics than those obtained by H.E.S.S. [69], we need more statistics and a larger energy coverage. We achieve that with the SEDs corresponding to 60 and 80 hours of observations, with an overall significance of about 11σ and 12.7σ respectively. Considering that the real zenith angle in which the source is visible from MAGIC is larger than the one used in the simulation, which only allows zenith angles up to 45 degrees, we consider that an observational proposal of 80 hours of observation is appropriate to research the nature of HESS J1828-099, but if it is not possible, with 60 hours the statistic is high enough to possibly perform the desired studies.

8. Conclusions

Considerando los capítulos previos, las conclusiones que extraemos sobre las binarias brillantes en gamma son: la clasificación en binarias de rayos gamma o binarias emisoras en gamma se ha hecho de acuerdo con las distribuciones de energía espectral; la dificultad de detectar el objeto compacto en algunas binarias de rayos gamma puede deberse a las propiedades geométricas del sistema y/o las condiciones medioambientales; las binarias emisoras en gamma son el sub-grupo más diverso; las cuestiones que quedan por resolver de cada binaria requieren un análisis más exhaustivo y/o instrumentación más sensible; los resultados obtenidos en el análisis de datos de PSR J2032+4127 son compatibles con los publicados en [32]; HESS J1828-099 puede detectarse con MAGIC con una alta significancia a partir de 60 horas de observación.

In this work, we performed exhaustive bibliographic research to understand and classify the different types of binaries systems in the HE and VHE regime. This research is complemented with an analysis of the VHE emission of the gamma-ray binary PSR J2032+4127 and with the expectations for detecting a new binary with MAGIC. Considering it, we can draw several conclusions from this work:

- Gamma-loud binaries can be classified into gamma-ray binaries or gamma-ray emitting binaries according to their SEDs, as shown in Chapters 4 and 5.
- The compact object of only three of the eight detected gamma-ray binaries is confirmed as a pulsar. The lack of pulsations or jets makes difficult the identification of the compact object in other systems. This can be due to geometrical properties and/or environmental conditions that make difficult the detection, which may require more sensitive instrumentation.
- Gamma-ray emitting binaries include microquasars, novae and colliding wind binaries, so it is the most diverse sub-class of gamma-loud binaries.
- There are still open questions for each gamma-loud binary, which requires deeper analysis and/or more sensitive instrumentation.
- The high-level data analysis of the gamma-ray binary *PSR J2032+4127* is compatible with that obtained in [32] despite the contamination from the nebula TeV *J2032+4127* in our results.
- The simulated SEDs for the gamma-ray binary candidate *HESS J1828-099* displayed that MAGIC could detect the source with high significance from 60 hours of observations.

As a general conclusion, despite the heterogenous sample that conforms to the gamma-loud binaries, this work has demonstrated that these systems present physical properties which allow us to classify them into two sub-groups. These groups share a property: each system is studied from the same perspective, evaluating the interaction of the two bodies that form the binary which produces the emission of gamma rays in each orbital period. The open questions related to gamma-loud binaries let us know that they could contribute as a great population involved in the most energetic phenomena in the Universe. With the development of more sensitive IACTs, we expect the discovery of more gamma-loud systems and, potentially, be able to answer some of these open questions.

9. References

- [1] Paredes, J.M. (2011), “Gamma-ray binaries: microquasars and binary systems with pulsar”, arXiv: 1101.4843.
- [2] Ribo, M. (2008). “TeV Gamma-ray astrophysics”, arXiv: 0801.2906.
- [3] Aharonian, F., et al. (2005a). “Discovery of the binary pulsar PSR B1259-63 in very-high-energy gamma rays around periastron with HESS”. *A&A*, 442, 1.
- [4] Aharonian, F., et al. (2005b). “Discovery of Very High Energy Gamma Rays Associated with an X-ray Binary”. *Science*, 309, 746.
- [5] Albert, J., et al. (2006). “Variable Very-High-Energy Gamma-Ray Emission from the Microquasar LS I +61 303”. *Science*, 312, 1771.
- [6] López Oramas, A. (2014). PhD Thesis “Multi-year campaign of the gamma-ray binary *LS I+61°303* and Search for VHE Emission from Gamma-Ray Binary Candidates with the MAGIC Telescopes”, Universitat Autònoma de Barcelona, ISBN: 9788449046421
- [7] Mirabel, I. F. (2006). “Very energetic gamma-rays from microquasars and binary pulsars”. *Science*, 312:1759.
- [8] Paredes, J.M., Bordas, P. (2019). “Phenomenology of gamma-ray emitting binaries”, arXiv: 1902.09898v1
- [9] Abdo, A. A., et al. (2011). “Discovery of High-energy Gamma-ray Emission from the Binary System PSR B1259-63/LS 2883 around Periastron with Fermi”. *ApJ Letters*, 736:L11.
- [10] Vasileiadis, G. and H.E.S.S. Collaboration (2005). “The H.E.S.S. experimental project”. *Nuclear Instruments and Methods in Physics Research A*, 553:268–273.
- [11] Chernyakova, M., et al. (2021). “Multi-wavelength properties of the 2021 periastron passage of PSR B1259-63”. arXiv:2106.03759
- [12] Chernyakova, M., et al. (2020). “New insight into the origin of the GeV flare in the binary system PSR B1259-63/LS 2883 from the 2017 periastron passage”. arXiv:2005.14060.
- [13] Yoneda, H., et al. (2023). “Unveiling properties of the non-thermal X-ray production in the gamma-ray binary LS 5039 using the long-term pattern of its fast X-ray variability”. *The Astrophysical Journal*, Volume 948, Issue 2, id.77, 13 pp.
- [14] Chernyakova, M., et al. (2020). “Gamma-ray binaries”. arXiv:2006.03615.
- [15] Abdo, A.A., et al. (2009). “Fermi LAT observations of LS I+61°303: First detection of an orbital modulation in GeV gamma rays”. *The Astrophysical Journal Letters*, Volume 701, Issue 2, pp. L123-L128.
- [16] Weng et al. (2022). “Radio pulsations from a neutron star within the gamma-ray binary LS I+61°303”. *Nature Astronomy*, Volume 6, p. 698-702.
- [17] Bednarek, W. (2011). “A model for the two component γ -ray spectra observed from the γ -ray binaries”. *MNRAS*, 418, L49
- [18] Gregory, P. C. (2002). “Bayesian Analysis of Radio Observations of the Be X-Ray Binary LS I +61°303”. *ApJ*, 575:427–434.
- [19] Ahnen, M. L., et al. (2016). “Super-orbital variability of LS I +61°303 at TeV energies”. *A&A*, 591, A76.
- [20] Aharonian, F. A., et al. (2007). “Discovery of a point-like very-high-energy γ -ray source in Monoceros”. *A&A*, 469, L1.
- [21] Malyshev, D. & Chernyakova, M. (2016). “Constraints on the spectrum of HESS J0632+057 from *Fermi*-LAT data”. *MNRAS*, 463,3074.
- [22] Adams, C.B., et al. (2021). “Observation of the gamma-ray binary H.E.S.S. J0632+057 with the H.E.S.S., MAGIC, and VERITAS telescopes”. arXiv:2109.11894.
- [23] Moritani, Y., et al. (2015). “Probing the Nature of the TeV γ -Ray Binary HESS J0632+057 by Monitoring Be Disk Variability”, *ApJL* 804 L32.

- [24] Barkov, M.V. and Bosch-Ramon, V. (2018). “A hydrodynamics-informed, radiation model for HESS J0632 + 057 from radio to gamma-rays”. *MNRAS*, 479, 1320.
- [25] Corbet, R. H. D., et al. (2011). “1FGL J1018.6-5856: a New Gamma-ray Binary”. *The Astronomer’s Telegram*, 3221.
- [26] H.E.S.S. Collaboration, Abramowski, A., Aharonian, F., et al. (2015). “Discovery of variable VHE γ -ray emission from the binary system 1FGL J1018.6–5856”. *A&A*, 577, A131.
- [27] Strader, J., et al (2015). “Optical Spectroscopy of the High-mass γ -Ray Binary 1FGL J1018.6-5856: A Probable Neutron Star Primary”. *ApJ*, 813, L26.
- [28] Corbet, R. H. D. et al. (2016). “A luminous gamma-ray binary in the Large Magellanic Cloud”. *ApJ*, 829, 105.
- [29] van Soelen, B. et al (2019). “The orbital parameters of the gamma-ray binary LMC P3”. *MNRAS*, 484, 4347.
- [30] Camilo, F. et al. (2009). “Radio Detection of LAT PSRs J1741-2054 and J2032+4127: No Longer Just Gamma-ray Pulsars”. *ApJ*, 705, 1.
- [31] Lyne, A., et al (2015). “The binary nature of PSR J2032+4127”. *MNRAS*, 451, 1.
- [32] Abeysekera, A.U. et al. (2018). “Periastron observation of TeV gamma-ray emission from a binary system with a 50-year period”. *The Astrophysical Journal Letters*, 867:L19.
- [33] HESS Collaboration, Abramowski, A. et al. (2015). “Discovery of the VHE gamma-ray source HESS J1832–093 in the vicinity of SNR G22.7–0.2”. *MNRAS*, 446, 1163.
- [34] Martí-Devesa, G. and Reimer, O. (2020). “X-ray and γ -ray orbital variability from the γ -ray binary HESS J1832-093”. *A&A*, 637, A23.
- [35] Carolina Pepe, Gabriela S. Vila, Gustavo E. Romero (2015). “Lepto-hadronic model for the broadband emission of Cygnus X-1”. *A&A*, 584, A95.
- [36] Brocksopp, C., et al. (1999). “Orbital, precessional and flaring variability of Cygnus X-1”. *MNRAS*, 309, 1063.
- [37] Brocksopp, C., Fender, R. P., & Pooley, G. G. (2002). “The orbital modulation in the radio emission of Cygnus X-1”. *MNRAS*, 336, 699.
- [38] Stirling, A. M., et al. (2001). “A relativistic jet from Cygnus X-1 in the low/hard X-ray state”. *MNRAS*, 327, 1273.
- [39] Zdziarski, A. A., Malyshev, D., Chernyakova, M., & Pooley, G. G. (2017). “High-energy gamma-rays from Cyg X-1”. *MNRAS*, 471, 3657.
- [40] Albert, J., et al. (2007). “Very High Energy Gamma-Ray Radiation from the Stellar Mass Black Hole Binary Cygnus X-1”. *ApJ*, 665, L51.
- [41] Ahnen, M.L., et al. (2017). “Search for very high-energy gamma-ray emission from the microquasar Cygnus X-1 with the MAGIC telescopes”. *MNRAS*, 472, 3.
- [42] Fermi LAT Collaboration, Abdo, A. A., et al. (2009). “Modulated High-Energy Gamma-Ray Emission from the Microquasar Cygnus X-3”. *Science*, 326, 1512.
- [43] Tavani, M., et al. (2009). “Extreme particle acceleration in the microquasar Cygnus X-3”. *Nature*, 462, 620.
- [44] Fernandez-Barral, A., et al. (2017). “Gamma rays from microquasars Cygnus X-1 and Cygnus X-3”. *arXiv:1709.01725*.
- [45] Fabrika, S., (2004). “The jets and supercritical accretion disk in SS433”. *Astrophys. Space Phys. Res.*, 12, 1.
- [46] Brinkmann, W., et al. (2007). “XMM-Newton observations of the eastern jet of SS 433”. *A&A*, 463, 611.
- [47] Abeysekera, A. U., et al. (2018). “Very high energy particle acceleration powered by the jets of the microquasar SS 433”. *Nature*, 562, 82.
- [48] Ahnen, M.L., et al. (2018). “Constraints of particle acceleration in SS433/W50 from MAGIC and H.E.S.S. observations”. *A&A*, 612, A14.
- [49] Olivera-Nieto, L. (2022). Gamma Conference “The jets of SS433 as seen by H.E.S.S.”.
- [50] Li, J., et al. (2020). “Gamma-ray heartbeat powered by the microquasar SS 433”. *Nature Astronomy*, 4.
- [51] Tibolla, O. on behalf of HAWC collaboration (2023). “Recent results from the HAWC experiment”. *J.Phys.: Conf. Ser.* **2429**012017.

- [52] López-Oramas, A., et al. (2022). “Prospects for Galactic transient sources detection with the Cherenkov Telescope Array”. arXiv:2108.03911.
- [53] Martí-Devesa, G., et al. (2020). “Hints of γ -ray orbital variability from γ^2 Velorum”. arXiv:2001.02708.
- [54] Martí-Devesa, G. and Reimer, O. (2021). “Eta Carinae with Fermi-LAT: Two full orbits and the third periastron”. *A&A*, 654, A44.
- [55] Tavani, M., et al. (2009). “Detection of gamma-ray emission from the Eta-Carinae region”. arXiv:0904.2736.
- [56] H.E.S.S. Collaboration (2020). “Detection of very-high-energy gamma-ray emission from the colliding wind binary Eta Carinae with H.E.S.S.”. *A&A*, 635, A167.
- [57] Abdo, A.A., et al. (2010). “Gamma-Ray Emission Concurrent with the Nova in the Symbiotic Binary V407 Cygni”. *Science*, 329, 5993.
- [58] Fermi-LAT Collaboration (2014). “Fermi establishes classical novae as a distinct class of gamma-ray source”. arXiv:1408.0735.
- [59] Acciari, V.A., et al. (2022). “Proton acceleration in thermonuclear nova explosions revealed by gamma rays”. *Nature Astronomy*, 6.
- [60] Cheung, C. C., Ciprini, S. & Johnson, T. J., (2021). “Fermi-LAT gamma-ray detection of the recurrent nova RS Oph”. *The Astronomer’s Telegram* 14834.
- [61] H.E.S.S. Collaboration (2022). “Time-resolved hadronic particle acceleration in the recurrent nova RS Ophiuchi”. *Science*, 376, 6588.
- [62] Aguasca-Cabot, A., et al. (2022). “The CTA-LST Project”. *PoS(Gamma2022)*055.
- [63] Aleksic, J., et al. (2016). “The major upgrade of the MAGIC telescopes, Part II: A performance study using observations of the Crab Nebula”. *Astroparticle Physics*, 72, 76-94.
- [64] Zanin, R., Carmona, E., Sitarek, J. (2013). “MARS, the MAGIC analysis and reconstruction software”, in *Proc. of the ICRC 2013 International Cosmic Ray Conference*, 2013.
- [65] Antcheva, I. Ballintijn, M., et al. (2011). ”ROOT A C++ framework for petabyte data storage, statistical analysis and visualization”, *Computer Physics Communications*, vol. 182, no. 6, pp. 1384-1385.
- [66] Otero Santos, J. (2018). Master Thesis “Unidentified Fermi Source (UFO) in an active galactic region”. *Facultad de Ciencias de la Universidad de La Laguna-Departamento de Astrofísica*.
- [67] Aliu, E., Anderhub, H, et al (2009). “Improving the performance of the single-dish Cherenkov telescope MAGIC through the use of signal timing”, *Astroparticle Physics*, vol. 30, no. 6, pp. 293-305.
- [68] T.-P. Li and Y.-Q. Ma (1983). “Analysis methods for results in gamma-ray astronomy”. *The Astrophysical Journal*, vol. 272, pp. 317-324.
- [69] H.E.S.S. collaboration (2018). “The H.E.S.S. Galactic plane survey”. arXiv:1804.02432
- [70] De Sarkar, A., et al. (2022). “Possible TeV gamma-ray origin of HESS J1828-099”. *The Astrophysical Journal Letters*, 927, 2, L35.